

Supplementary Materials for

ECM-inspired micro/nanofibers for modulating cell function and tissue generation

Yun Xu, Guodong Shi, Jincheng Tang, Ruoyu Cheng, Xiaofeng Shen, Yong Gu, Liang Wu, Kun Xi, Yihong Zhao,
Wenguo Cui*, Liang Chen*

*Corresponding author. Email: wgcui80@hotmail.com (W.C.); chenliang1972@sina.com (L.C.)

Published 25 November 2020, *Sci. Adv.* **6**, eabc2036 (2020)
DOI: 10.1126/sciadv.abc2036

This PDF file includes:

Figs. S1 to S7
Tables S1 to S3

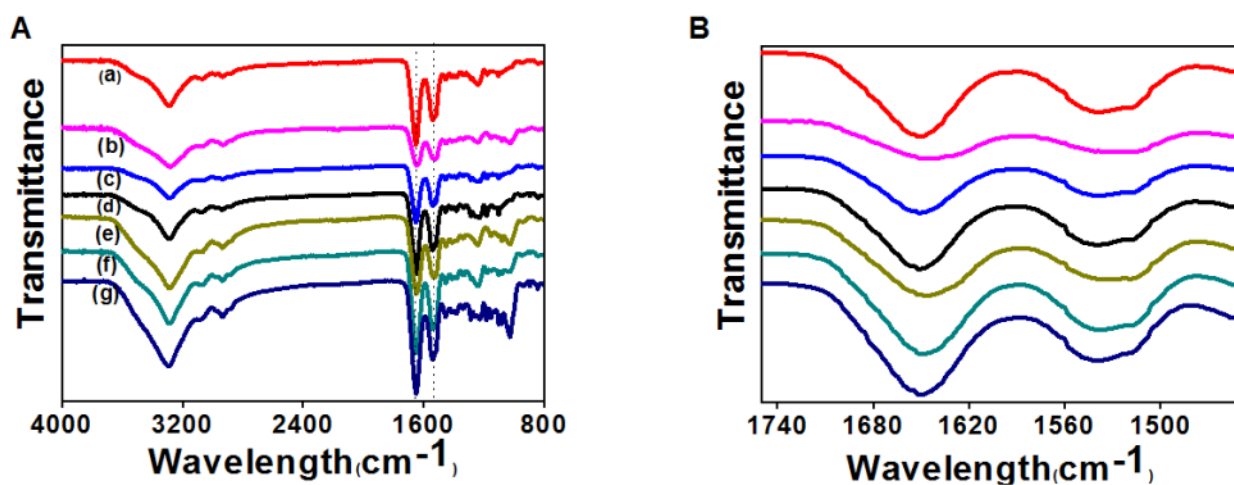


fig. S1. FTIR characterization of fibers containing varying COL-I ratios. A: The FTIR spectra of SF-Col-I fibers containing varying Col-I content. B: Magnified region of FTIR spectra from SF-Col-I fibers containing varying Col-I content. (a. SF : Col-I ratio 100:0%; b. SF : Col-I ratio 95:5%; c. SF : Col-I ratio 90:10%; d. SF : Col-I ratio 85:15%; e. SF : Col-I ratio 80:20%; f. SF : Col-I ratio 75:25%; SF : Col-I ratio 50:50%)

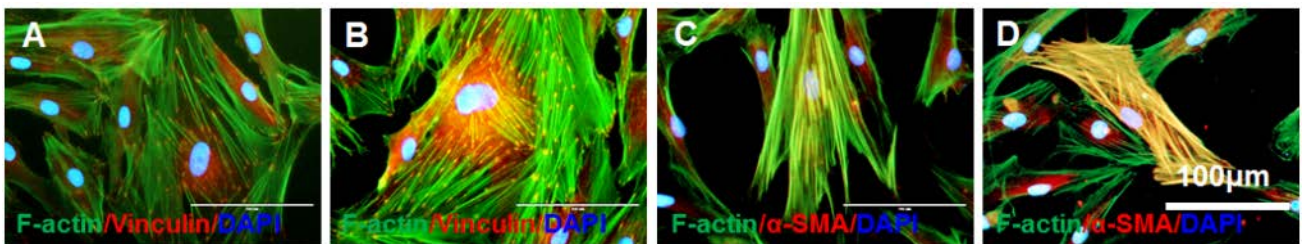


fig. S2. Phenotype of human skin fibroblasts and human skin keloid fibroblasts. A: Human skin fibroblasts stained by vinculin (red); B: human skin keloid fibroblasts stained by vinculin (red), C: Immunofluorescence staining for the expression of α -SMA in human skin fibroblasts; D: Immunofluorescence staining for the expression of α -SMA in human skin keloid fibroblasts. F-actin stained by phalloidin (green) DAPI (blue).

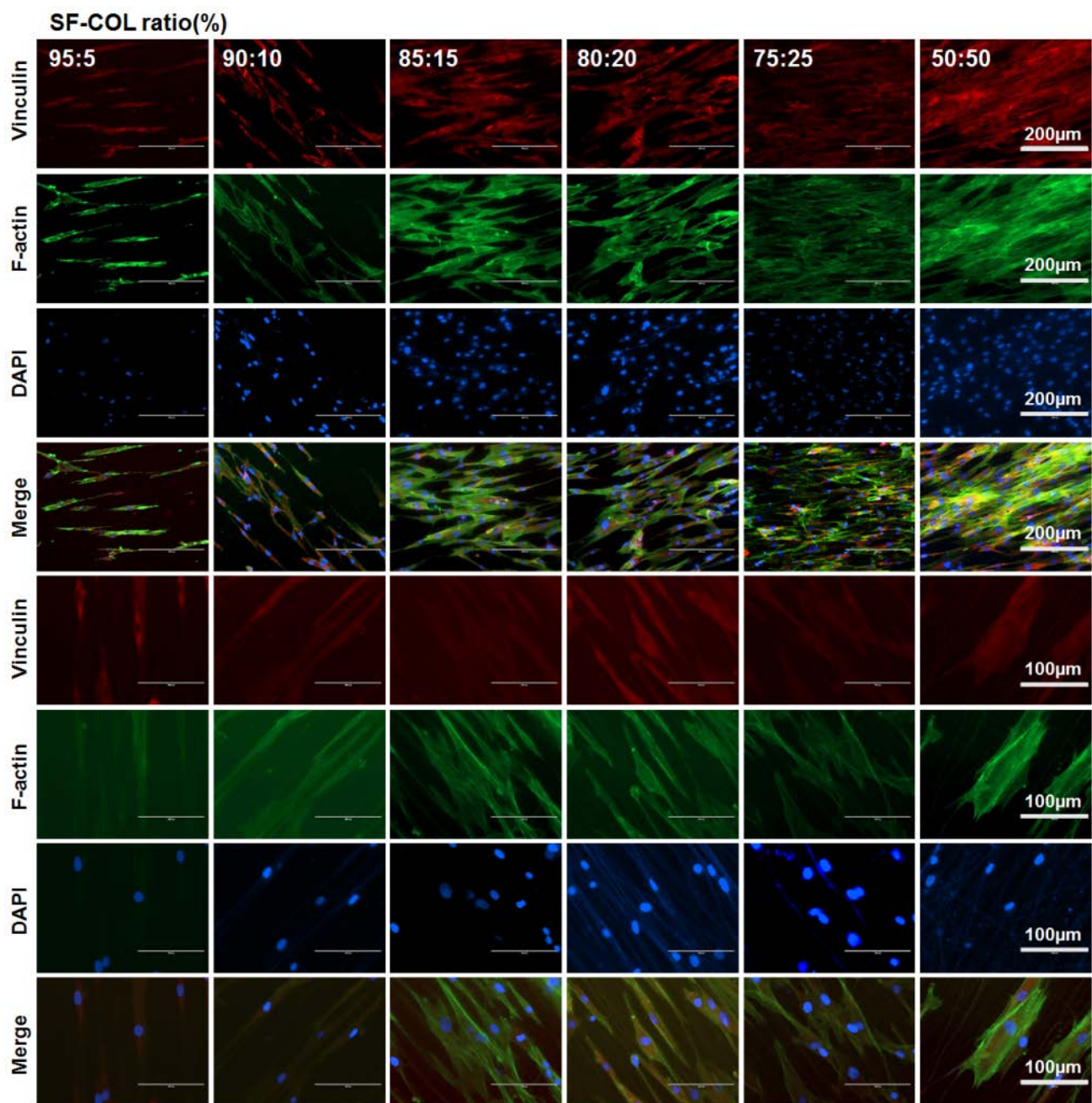


fig. S3. Immunofluorescence staining of vinculin in cells cultured on ASCF containing varying COL-I content.

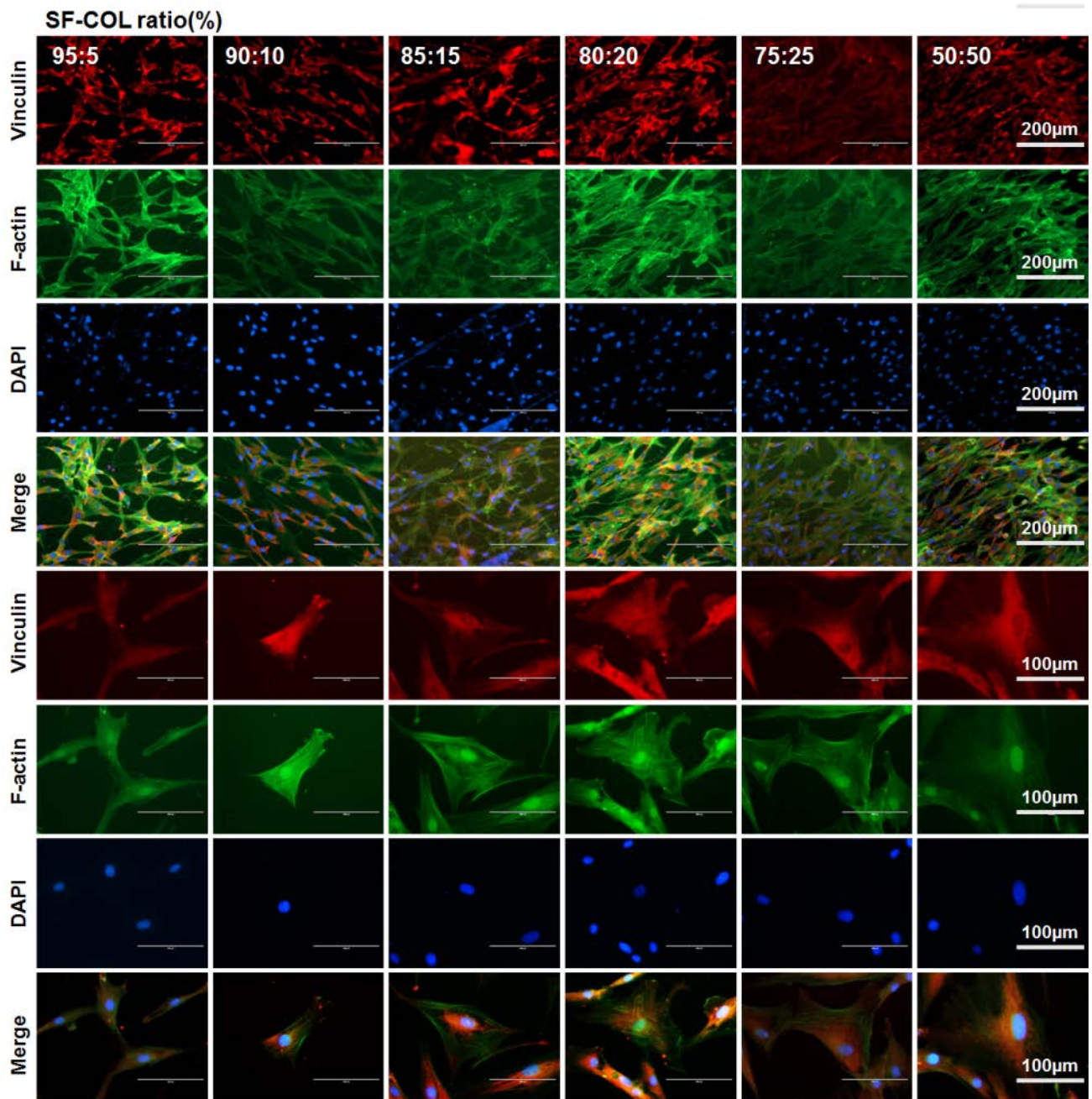


fig. S4. Immunofluorescence staining of vinculin in cells cultured on RSCF containing varying COL-I content.

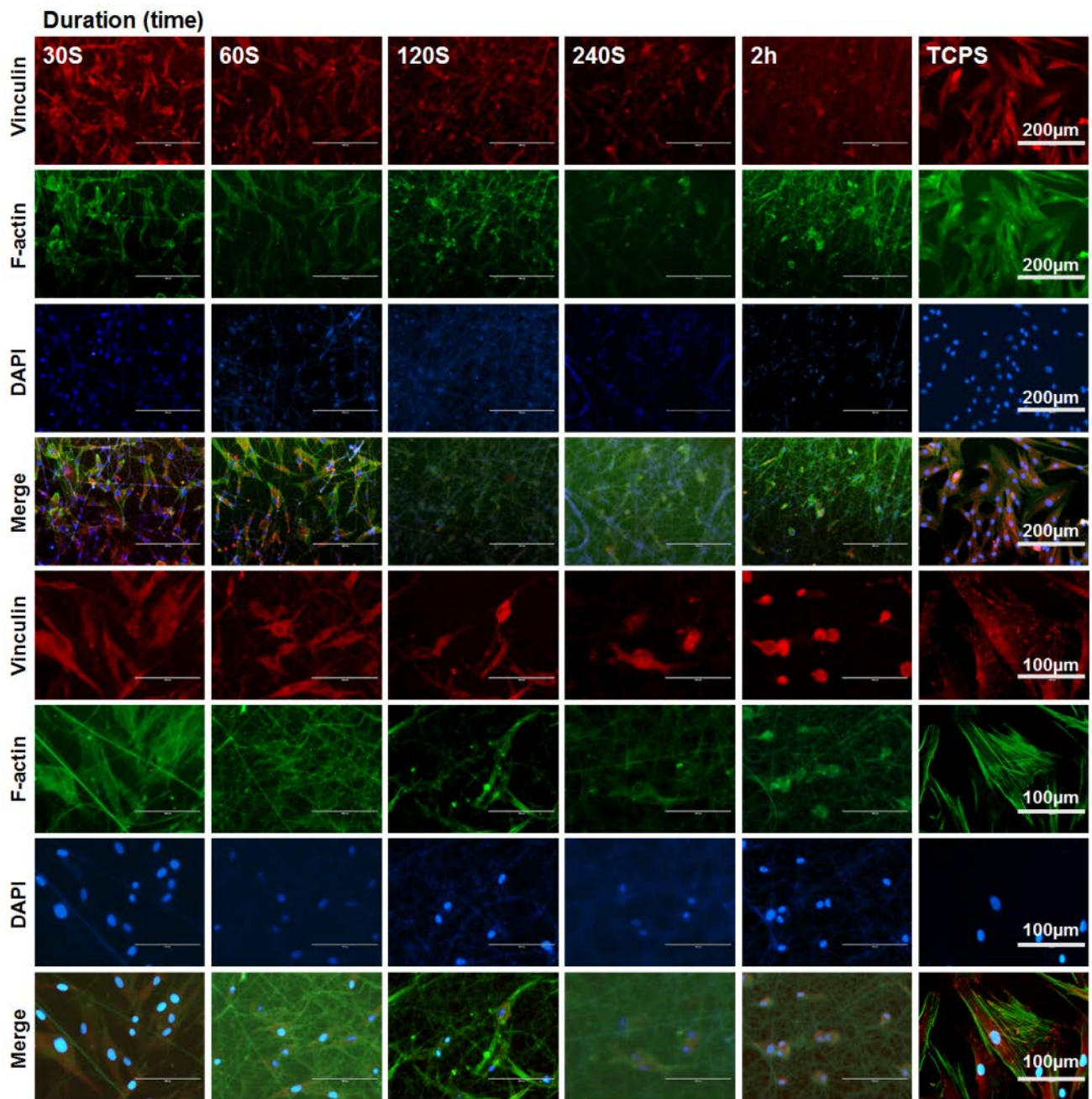


fig. S5. Immunofluorescence staining of vinculin in cells cultured on RSF with different fiber densities

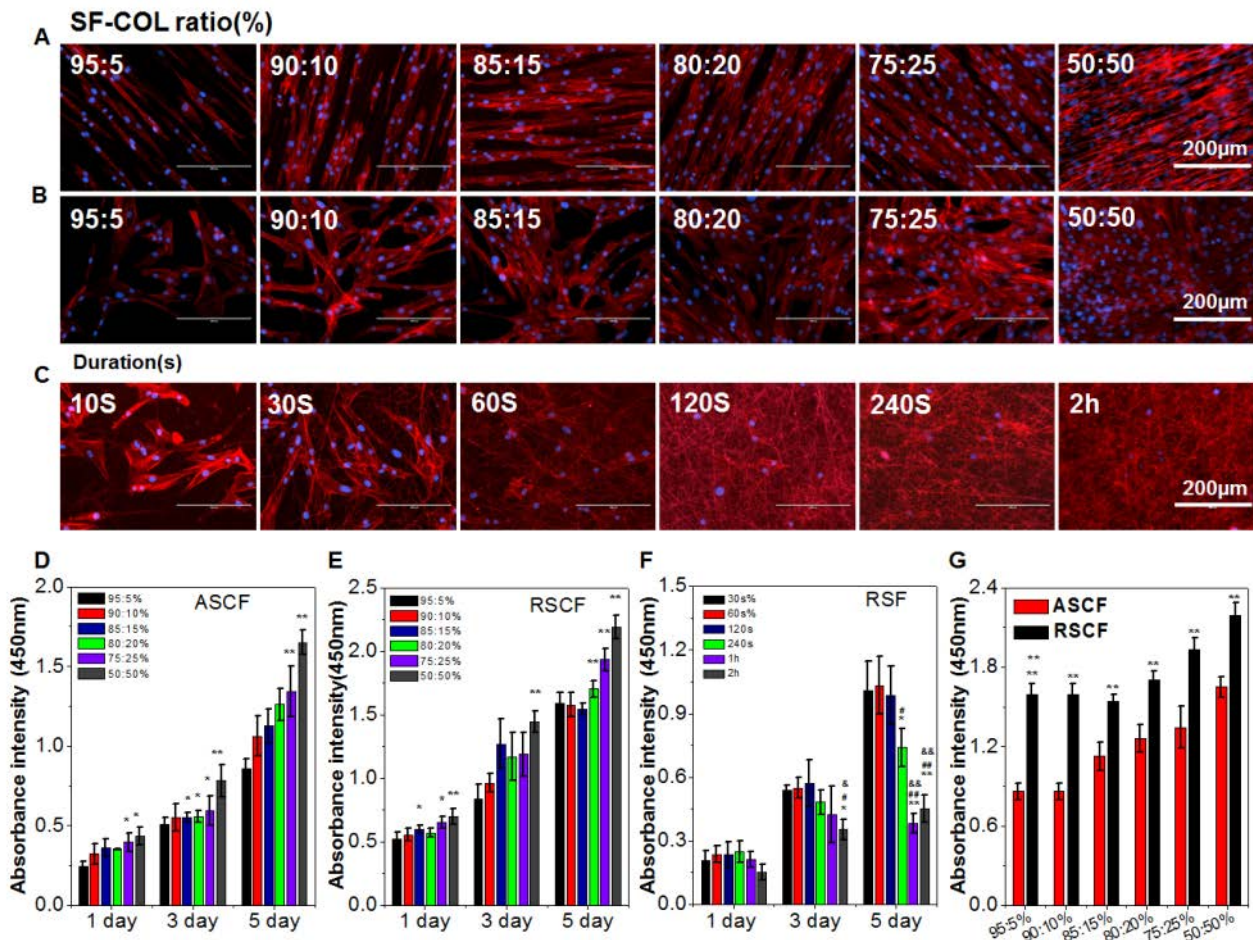


fig. S6. Cytoskeleton staining and proliferation rate of fibroblasts and myofibroblasts cultured on fibers. (A-B): Cytoskeleton staining of fibroblasts cultured on (A) ASCF and (B) RSCF containing gradient COL-I ratios; (C): Cytoskeleton staining of myofibroblasts cultured on RSF with different fiber densities. (D-G): Cell viability determined by CCK-8 assay; CCK-8 assay of fibroblast cultured on (D) ASCF and (E) RSCF containing gradient COL-I ratios. (F): CCK-8 assay of myofibroblast cultured RSF with different fiber densities. (G): Comparison on proliferation rate of fibroblasts cultured on ASCF and RSCF under same COL-I content at day 5 of cell culture. Statistically significant differences were indicated by* $p < 0.05$, ** $p < 0.01$ when compared with the 95:5% group (D,E); Statistically significant differences were indicated by* $p < 0.05$, ** $p < 0.01$ indicated that compared with the 30s group, # $p < 0.05$, ## $p < 0.01$ indicated that compared with the 60s group, & $p < 0.05$, && $p < 0.01$ indicated that compared with the 120s group (F); Statistically significant differences were indicated by * $p < 0.05$, ** $p < 0.01$ when comparing between ASCF and RSCF groups (G).

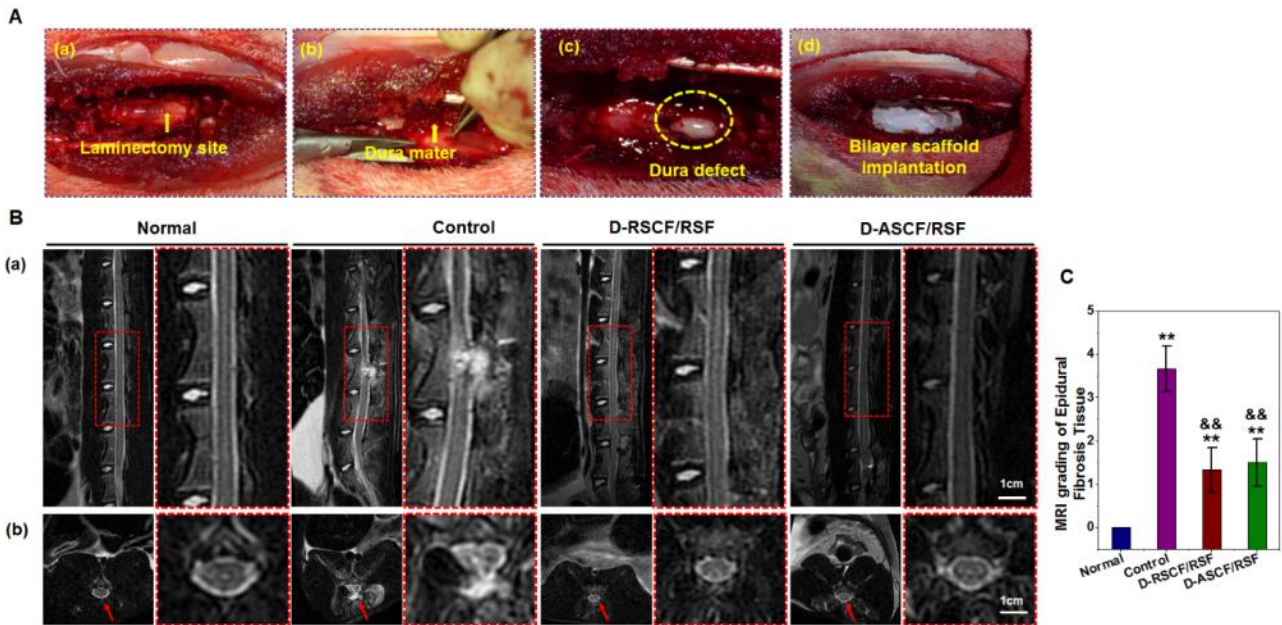


fig S7. The detail of surgical procedure and MRI images after 8 weeks after surgery. (A) The detail of surgical procedure. (A. a) A midline skin incision was made to expose L5 laminae and the total laminectomy was performed on L5; (A. b) Yellow arrow indicated that intact dura mater prior to tissue excision. Scissor excision of dura mater; (A. c) An elliptical dura mater defect (11 ×3 mm) was established. (A. d) Dural defect reconstructed and covered with a bilayer heterogeneous micro/nano fiber scaffold. (B)MRI images. (B a) T2 weighted MRI images of the spine section 8 weeks after surgery with (a) sagittal and (B b) transverse section. (Yellow arrow refers to the adhesion of the scar tissue to the spinal cord and the infiltration in the spinal canal.) (C). Quantification analysis of fibrosis at focal area by MRI grading. Statistically significant differences were indicated by * $p < 0.05$ ** $p < 0.01$ when compared with normal group, and & $p < 0.05$ && $p < 0.01$ when compared with the control group. Data are expressed as mean \pm SD for six samples per group.

Table S1. MRI grading of epidural scar adhesions

0	no scar
1	0 > to ≤ 25 % of the quadrant filled with scar
2	>25 to ≤ 50 % of the quadrant filled with scar
3	>50 to ≤75 % of the quadrant filled with scar
4	>75 to ≤100 % of the quadrant being filled with scar

Table S2. Rydell–BAalaz standard

1	Absence of adhesion between paraspinal muscles and dura matter, with near normal separation plane of tissues
2	Mild-to-moderate adhesion, and separation of epidural fibrosis from dura matter was easy by a dissector
3	Severe adhesion, and separation of epidural fibrosis from dura matter was hard or impossible by a dissector

Table S3. Histological evaluation of epidural adhesions

0	The dura mater was free of scar tissue
1	Only thin fibrous bands between scar tissue and dura mater were observed
2	Continuous adherence was observed but was less than two thirds of the laminectomy defect
3	Scar tissue adherence was large, more than two thirds of the laminectomy defect, and/or extended to the nerve roots